UDC 621.4
DOI: 10.15587/2706-5448.2025.326746

Oleksandr Zhevzhyk,
Iryna Potapchuk,
Vadym Horiachkin,
Serhii Raksha,
Dmytro Bosyi,
Andrii Reznyk

MATHEMATICAL MODELLING OF MIXTURE FORMATION IN THE COMBUSTION CHAMBER OF A DIESEL ENGINE

The object of research is the process of fuel mixture formation in a vortex combustion chamber located in the piston of a diesel engine.

Ineffective mixture formation leads to increased specific fuel consumption and harmful emissions into the atmosphere. The research addresses determining the conditions under which complete evaporation of droplets is achieved and the required ratio of the amount of fuel vapor and the available amount of air depending on the piston radius.

A mathematical model was created to describe the behavior of fuel droplets under the influence of aerodynamic forces, heat transfer, and phase transition processes. The calculations determined the radial fuel vapor concentration and air-fuel ratio distribution. The study found that fuel droplets with sizes ranging to 90.7 μm are completely evaporated which contributes to volumetric mixture formation. The model also identified regions where the mixture reaches stoichiometric conditions necessary for autoignition, particularly at a radius of $r/R_c = 0.22$.

This is explained by the rapid evaporation of small droplets, the number of which, as a function of the diameter distribution, is the majority, and their high speeds of movement relative to air and high mass transfer coefficients in the initial spraying area.

The study demonstrates that despite non-uniform fuel vapor distribution, volumetric mixture formation is achieved. The interaction between fuel droplets and the swirling air motion ensures adequate mixing, facilitating complete and efficient fuel combustion.

The results can be applied to optimize diesel engine designs by improving combustion chamber geometry and fuel injection strategies. The model is particularly useful for engines with high-pressure fuel injection systems. The work results contribute to developing more efficient diesel engines that comply with stricter emission regulations.

Keywords: *droplet movement, evaporation, mixture formation, spray dispersion, volumetric combustion, excess air, steam unevenness.*

Received: 13.01.2025
Received in revised form: 09.03.2025
Accepted: 01.04.2025
Published: 16.04.2025

How to cite
Zhevzhyk, O., Potapchuk, I., Horiachkin, V., Raksha, S., Bosyi, D., Reznyk, A. (2025). Mathematical modelling of mixture formation in the combustion chamber of a diesel engine. Technology Audit and Production Reserves, 2 (1 (82)), 63–68. https://doi.org/10.15587/2706-5448.2025.326746

1. Introduction

The problem of mixture formation occupies a significant place in the scientific specialized research of major research centers in the United States, Western Europe and China, because its solution allows to minimize specific fuel engine consumption in each case.

The consequence of the unresolved issue of proper air-fuel mixing in diesel internal combustion engines is harmful emissions, namely carbon monoxide, nitrogen oxides, unburned hydrocarbon components of the fuel, and the emission of fine particulate carbon [1, 2]. These emissions pose a significant threat to human health and the environment [3, 4].

Nowadays, for finding optimal solutions to improve mixture formation in internal combustion chambers, workflow modeling is performed using modern specialized software systems such as KIVA [5], AVL FIRE™ M [6], VECTIS [7], ANSYS [8] and many others.

In [9], a new piston shape for a low-power diesel engine is proposed, featuring a sharp stepped edge with deep penetration and radial protrusions on the inner surface of the combustion chamber. The authors aim to improve mixture formation and fuel jet combustion speed through the chamber's geometry. As noted by the authors themselves, the modeling results are only qualitatively confirmed. It is also important to note that the use of jet-type injectors does not eliminate radial non-uniformity and, to improve fuel dispersion, requires small nozzle holes and high injection pressure.

In [10], a mathematical model was developed to calculate the averaged thermodynamic parameters in the engine's combustion chamber. This model allows determining average pressure, temperature, the amount of combustion products, power output, and other variables as functions of the crankshaft rotation angle. However, the model does not account for local variations in the calculated quantities, spray dispersion, or droplet evaporation processes, which are essential for further optimization of the combustion chamber and piston design.

Due to the complexity of organizing volumetric mixture formation, [11] investigated the interaction between fuel droplets and the cylinder and piston walls. The research, conducted using a CFD model, identified the optimal injection timing for such spray processes. However, the conditions for achieving volumetric mixture formation – crucial for the most efficient fuel combustion – remain unclear.

In [12], experimentally, and in [13], using numerical modeling, jet spraying of liquids (diesel fuel, e-fuels, biofuels) using diesel injectors was studied, with the results compared to known calculation formulas. The shape and penetration depth of the fuel jet were determined. In [13], spline-like dependencies for jet penetration length were obtained, which may exhibit several extrema; parabolic and linear profiles are also possible. The evaporation process of fuel

ISSN-L 2664-9969; E-ISSN 2706-5448

within the spray plume is planned for future investigations by the authors of [12].

Despite significant efforts in modeling processes within the diesel engine cylinder, ongoing generalizations and proposals for new designs and strategies continue to emerge, aiming to achieve near-zero emissions and reduced fuel consumption. These strategies, despite their drawbacks, have the potential to enhance mixture formation efficiency in the engine and reduce harmful exhaust emissions to meet future regulations [14].

The main trends in improving combustion chambers (CC) include increasing air velocity and its turbulence, creating a continuous fuel film on the walls or atomizing fuel at pressures up to 130 MPa and higher, with an increased proportion of droplets burning in the volume. Turbulence is achieved by imparting rotational motion to the air around the axis of the combustion chamber.

The subject of research and mathematical modelling in well-known works was the volumetric mixture formation in an undivided and semi-divided combustion chamber. Approaches to building a mathematical model (numerical study of a sprayed fuel plume or a combustion chamber with fuel injection) require knowledge of the air velocity field.

In [15], a vortex combustion chamber in the piston and a pneumomechanical injector (Fig. 1) with enhanced mixture formation control capabilities were proposed for the SN-6D-11 engine. This engine was used for autonomous power generators and was mass-produced in Ukraine. A centrifugal fuel atomizer was designed for this combustion chamber, operating at a pressure starting from 16 MPa (while the injection start pressure in the serial engine is 20.6 MPa).

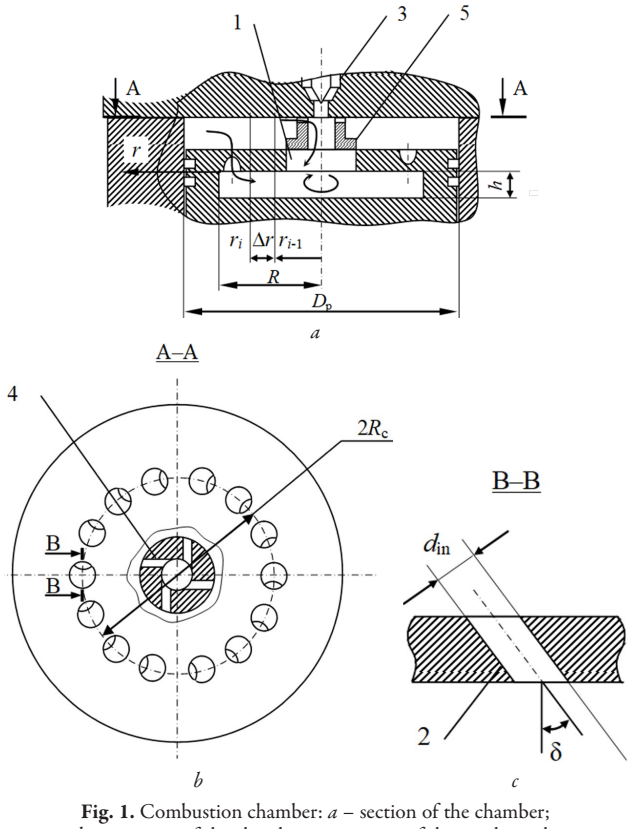

Fig. 1. Combustion chamber: *a* – section of the chamber; *b* – top view of the chamber; *c* – section of the air channels

After the central channel 1 is closed, the main air mass enters the combustion chamber through the inclined channels 2 and rotates around the axis. Fuel is injected through a centrifugal nozzle 3 in the form of a conical spray, and larger droplets are fragmented by the swirling airflow entering from the space above the piston via tangential channels 4 in the swirler 5.

The aim of the study is to build a mathematical model and perform calculations of the mixing process in the combustion vortex chamber, which is located in the piston (Fig. 1). This will allow optimizing the design of diesel engines by improving the geometry of the combustion chamber and the fuel injection strategy.

2. Materials and Methods

2.1. A physical representation of fuel combustion

The excess air factor determines the perfection of the fuel combustion apparatus and its efficiency. The maximum temperature is achieved at the stoichiometric mass ratio of air and fuel vapor in the combustion chamber:

$$\frac{G_a}{G_v}=\pm l_0, \tag{1}$$

where G_a and G_v are the masses of air and fuel vapor, respectively; α is the air excess ratio; and l_0 is the theoretically required amount of air for the combustion of 1 kg of fuel.

For film and bulk-film combustion in the combustion chamber, condition (1) is not feasible. In volumetric combustion, mixture formation with a minimum deviation from (1) is achieved by choosing the shape and size of the combustion chamber with the adopted fuel spray.

The height of the vortex chamber with flat end walls does not vary along the radius. Since the air density in the combustion chamber remains practically constant for a fixed time, the share of air in the i-th annular volume of thickness r_i–r_{i-1} with an average radius $r_{cpi}=0.5(r_{i-1}+r_i)$ is given by:

$$G_{a\,i}=\frac{r_i^2-r_{i-1}^2}{R^2}G_a. \tag{2}$$

In an arbitrary annular volume, there will be a mixture of evaporating and fully evaporated droplets. The mass of fuel evaporated from droplets with a diameter $d_{j,i}$ in each ring can be expressed as:

$$G_{v\,j,i}=\frac{1}{6}\pi(\bar{d}^3_{j,i-1}-\bar{d}^3_{j,i})\rho_f n_j. \tag{3}$$

The parameters $\bar{d}_{j,i-1}$, $\bar{d}_{j,i}$ represent the average diameter of droplets at the boundary between radii r_i and r_{i-1}, within the size range d_{j-1} to d_j, which corresponds to the intervals used to divide the droplet size distribution function. The quantity n_j is the number of droplets with an initial average diameter $\bar{d}_j$. If a droplet in the annular region r_{i-1}–r_i has completely evaporated, then $d_{j,i}=0$.

The number of droplets n_j with an average diameter $\bar{d}_j$ is determined using the differential $v(d)$ or integral $V(d)$ mass distribution function for droplets in the injector spray (Fig. 2). To achieve this, the mass distribution function is divided into intervals $d_{j-1}...d_j$ with an average diameter $\bar{d}_j=0.5(d_{j-1}+d_j)$. The fraction of droplet mass corresponding to the interval d_{j-1} to d_j is expressed as:

$$\Delta V_j=\int_{d_{j-1}}^{d_j} v(d)\mathrm{d}d. \tag{4}$$

The calculations use a one-parameter distribution with an integral characteristic:

$$V(d)=\frac{2\beta}{3\pi}\int_0^d d^3K_1(\beta d)\mathrm{d}d, \tag{5}$$

where $K_1(\beta d)$ is the Bessel function.

The parameter β is determined using one of the median droplet diameter (d_m) $\beta=3.05/d_m$ or the Sauter volume-to-surface mean

diameter $(d_{32})\ \beta = 3\pi/(4d_{32})$ or the maximum diameter $(d_{max})\ \beta = 7/d_{max}$, corresponding to the cumulative distribution function value $V = 0.95$.

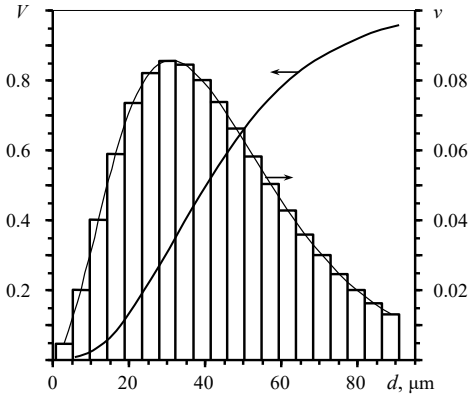

Fig. 2. Differential and integral functions of droplet size distribution

The mass of fuel with an average initial droplet diameter $\bar{d}_{0j}$ within the interval d_{j-1}, d_j can be calculated as:

$$G_{fj} = \Delta V_j G_f. \quad (6)$$

The parameter G_f represents the total mass of the injected fuel.

On the other hand, the mass of fuel droplets with an average initial diameter $\bar{d}_{0j}$:

$$G_{fj} = \frac{1}{6}\pi \bar{d}_{0j}^3 \rho_f n_j. \quad (7)$$

Then, from (6) and (7):

$$n_j = 6\frac{\Delta V_j G_f}{\pi \bar{d}_{0j}^3 \rho_f}, \quad (8)$$

and from (3) and (8), the mass of fuel evaporated from droplets with a diameter $d_{j,i}$ in the ring is:

$$G_{vj,i} = \frac{\bar{d}_{j,i-1}^3 - \bar{d}_{j,i}^3}{\bar{d}_{0j}^3}\Delta V_j G_f. \quad (9)$$

The total mass of vapor in the ring with radii r_i, r_{i-1} from droplets of all diameters can be expressed as:

$$G_{vi} = \sum_{j=1}^{N}\frac{\bar{d}_{j,i-1}^3 - \bar{d}_{j,i}^3}{\bar{d}_{0j}^3}\Delta V_j G_f, \quad (10)$$

where N is the number of diameter intervals into which the droplet size distribution function is divided.

Then, from (2), (10), and (1), the local value of the air-to-fuel vapor mass ratio in the volume of the ring, can be determined as $G_{ai}/G_{vi} = \alpha_i l_0$.

As well as the local specific air excess ratio can be determined as:

$$\alpha^* = \frac{\alpha_i}{\alpha} = \frac{r_i^2 - r_{i-1}^2}{R^2}\Bigg/\sum_{j=1}^{N}\frac{\bar{d}_{j,i-1}^3 - \bar{d}_{j,i}^3}{\bar{d}_{0j}^3}\Delta V_j, \quad (11)$$

where includes the diameter d_j, which is determined numerically by solving the system of equations of motion and evaporation of droplets.

2.2. Equation of motion of a droplet in cylindrical coordinate system

The scheme for calculating the movement of drops is shown in Fig. 3.

Let's consider fuel droplets as those that deform with variable mass. Vapor escape from the droplet is uniform across its surface.

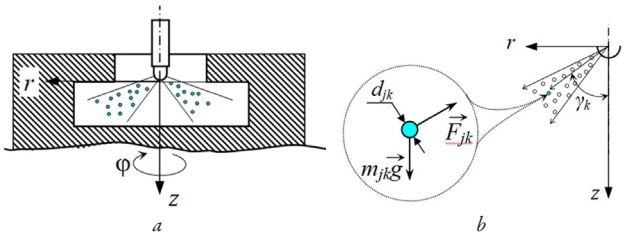

Fig. 3. Scheme for calculating: *a* – the movement of drops in the chamber; *b* – the forces acting on a drop

Equation of motion of the center of mass of the j-th droplet, which exits the nozzle at angles γ_k:

$$m\frac{d\vec{V}_{jk}}{d\tau} = -\vec{F}_{jk} + m_{jk}\vec{g}, \quad (12)$$

where $m_{jk} = \pi d_{jk}^3 \rho_f / 6$ is droplet mass, $\vec{\theta}_{jk} = \{V_{jk}, W_{jk}, U_{jk}\}$ is droplet velocity vector, d_{jk} is droplet diameter, ρ is fuel density, τ is time.

Aerodynamic drag force of the droplet:

$$\vec{F}_{jk} = -\frac{s_{jk}}{2}C_{jk}\psi_{jk}\rho_{mix}|\vec{\theta}_{jk} - \vec{\vartheta}|(\vec{\theta}_{jk} - \vec{\vartheta}) + m_{jk}\vec{g}, \quad (13)$$

where ρ_{mix} density of the mixture of moist air and fuel vapor, $\vec{\vartheta} = \{\upsilon, w, u\}$ is air velocity. The area of the droplet midsection $s_{jk} = \pi d_{jk}^2/4$.

Thus, the droplet motion equations in a vortex chamber in the coordinate system r,j,z are written as follows:

$$\begin{aligned}
&m_{jk}\left(\frac{dV_{jk}}{d\tau} - \frac{W_{jk}^2}{r}\right) = -\frac{s_{jk}}{2}C_{jk}\psi_{jk}\rho_{mix}|\vec{\theta}_{jk} - \vec{\vartheta}|(V_{jk} - \upsilon);\\
&m_{jk}\left(\frac{dW_{jk}}{d\tau} - \frac{V_{jk}W_{jk}}{r}\right) = -\frac{s_{jk}}{2}C_{jk}\psi_{jk}\rho_{mix}|\vec{\theta}_{jk} - \vec{\vartheta}|(W_{jk} - w);\\
&m_{jk}\frac{dU_{jk}}{d\tau} = -\frac{s_{jk}}{2}C_{jk}\psi_{jk}\rho_{mix}|\vec{\theta}_{jk} - \vec{\vartheta}|(U_{jk} - u) + m_{jk}g;\\
&V_{jk} = \frac{dr_{jk}}{d\tau};\ W_{jk} = \frac{r_{jk}d\varphi_{jk}}{d\tau};\ U_{jk} = \frac{dz_{jk}}{d\tau}.
\end{aligned} \quad (14)$$

The coefficient of aerodynamic drag of the ball will be determined according to the formula [16]:

$$C_{jk} = \frac{24}{\mathrm{Re}_{jk}} + \frac{4.4}{\sqrt{\mathrm{Re}_{jk}}} + 0.32, \quad (15)$$

which is valid when $\mathrm{Re}_{jk} = \frac{\rho_{mix}|\vec{\theta}_{jk} - \vec{\vartheta}|d_{jk}}{\mu_{mix}}$ in the range of $Re_{jk} < 6\cdot 10^3$.

The effect of the droplet deformation on the effective area of the midsection is taken into account by the deformation coefficient [17]:

$$\psi_{jk} = \exp\left(0.03We_{jk}^{1.5}\right), \quad (16)$$

where the Weber number $We_{jk} = \frac{\rho_{mix}d_{jk}|\vec{\theta}_{jk} - \vec{\vartheta}|^2}{\sigma_{jk}}$.

The equation of equilibrium evaporation of a droplet in a flow, according to [17], is written in the form:

$$\frac{d}{d\tau}d_{jk}^2 = \frac{8\rho_{mix}D_v}{\rho_f}\left(1 + 0.3\bar{\varphi}\sqrt{\mathrm{Re}_{jk}\,\mathrm{Pr}}\right)\ln\frac{1 - C_v}{1 - C_{vs}}, \quad (17)$$

where $\mathrm{Pr}_{mix} = \nu_{mix}/a_{mix}$ is the Prandtl number, $C_v = 1\Big/\frac{M_a}{M_v}\left(\frac{P}{P_v} - 1\right) + 1$, $a_{mix} = \lambda_{mix}/(c_{p\,mix}\cdot\rho_{mix})$ is the coefficient of thermal conductivity.

The effect of heat transfer on evaporation in the flow is taken into account by the coefficient:

ISSN-L 2664-9969; E-ISSN 2706-5448

$$\bar{\varphi}=\left[\frac{Nu_w}{2}\left(\frac{1-C_v}{1-C_{vs}}\right)^{\mathrm{Pr}_d}\right]^{-0.5},$$

$$Nu_w=2\mathrm{Pr}_d\left[\left(\frac{1-C_v}{1-C_{vs}}\right)^{\mathrm{Pr}_d}-1\right]^{-1}\ln\frac{1-C_v}{1-C_{vs}},$$

where $\mathrm{Pr}_d=D_v/a_{mix}$ is the diffusion Prandtl number.

Energy conservation equation of an evaporating droplet can be determined as:

$$m_{jk}\frac{d}{d\tau}h_{jk}=\alpha_{fjk}\left(T-T_{fjk}\right)\pi d_{jk}^2+\frac{d}{d\tau}m_{jk}L_{jk}, \quad (18)$$

where $h_{jk}=c_{fjk}T_{fjk}$ is the enthalpy of a droplet; T_{fjk} is the temperature of a droplet; c_{fjk} is the heat capacity of a droplet; L_{jk} is the specific heat of fuel evaporation.

The heat transfer coefficient is:

$$\alpha_{fjk}=\frac{Nu\lambda_{mix}}{d_{jk}},$$

and the Nusselt number is:

$$Nu=Nu_w\left(1+0.3\bar{\varphi}\sqrt{\mathrm{Pr}_{mix}\,\mathrm{Re}_{jk}}\right).$$

The distribution of air velocity in the vortex combustion chamber (CC) was obtained in [18]. The initial conditions for the equations of motion for air and evaporating droplets are determined based on thermodynamic relationships, depending on the degree of air compression in the CC and the parameters of fuel injection.

2.3. Thermophysical properties of interacting phases

The fuel droplets moving in the chamber are surrounded by a multi-component environment consisting of fuel vapor and air. The thermophysical properties of this environment will determine the aerodynamic drag force, heat and mass transfer of the evaporating droplet.

The thermal properties of fuel, steam and air are calculated using the average temperature $T_{av}=(T_f+T)/2$.

Motor fuel [16]: density, kg/m^3 $\rho_f=1000\,d_4^t$; $d_4^t=d_4^{20}+\beta(20-t_f)$; $\beta=0.000712$, K^{-1}; d_4^{20} is the ratio of the fuel density at a temperature of 20 °C to the density of water at 4 °C; t_f is the fuel temperature, °C.

Molecular mass:

$$M=(7K-21.5)+(0.76-0.04K)t_s+(0.0003K-0.00245)t_s^2,$$

where the factor characterizing the change of paraffin hydrocarbons in the fuel is $K=1.216\sqrt[3]{T_s/d_{15}^{15}}$; T_s and t_s are the average molecular boiling temperature of the fuel at K and °C.

Surface tension, N/m:

$$\sigma=\sigma_0\left(1-\frac{T_f}{T_{cr}}\Big/1-\frac{T_0}{T_{cr}}\right),$$

where critical temperature (°C) $t_{cr}=82+0.97z-0.00049z^2$, where $z=(1.8t_s+132)d_4^{15}$; σ_0 – the value of surface tension at a temperature of T_0.

Heat of vaporization, kJ/kg:

$$L=\frac{4.187}{d_4^{15}}\left(60-0.09t_s\right).$$

Heat capacity (kJ/kg) in the temperature range of t_f=0–200 °C:

$$c_f\Big|_0^t=\frac{1.7}{\sqrt{d_{15}^{15}}}\left(1+10^{-3}t_f\right).$$

Vapor of motor fuel [16].

Saturated vapor pressure, MPa:

$$P_v=0.098\cdot10^{4.186-\frac{2050}{T_v}},$$

where T_v is the fuel vapor temperature.

Diffusion, m^2/s:

$$D_v=D_{v0}\left(\frac{T}{T_0}\right)^2\frac{P_0}{P}.$$

Dynamic viscosity, Pa×s:

$$\mu_v=\mu_{v0}\frac{T}{T_0},\quad \mu_{v0}=22.5\cdot10^{-5}\frac{\sqrt{M}\sqrt[3]{P_{cr}}}{T_{cr}}-0.65\cdot10^{-5},$$

where P_{cr} is the critical pressure in atm.

At critical values of pressure and temperature, the difference between the liquid and gaseous states of matter disappears. For motor fuels, which are mixtures of hydrocarbons, the critical parameters are determined by the mean effective values [16].

Heat capacity, kJ/(kg·K):

$$c_{pv}=\frac{4-d_{15}^{15}}{1540}\left(1.8t+702\right)\left(0.146K-0.41\right).$$

Thermal conductivity, W/(m·K):

$$\lambda_v=\lambda_{v0}\left(\frac{T}{T_0}\right)^2,\quad \lambda_{v0}=6.3\mu_{v0}c_{pv0}.$$

Air [16]: dynamic viscosity according to the formula, Pa×s:

$$\mu_a=\mu_{a0}\frac{273.2+C}{T+C}\left(\frac{T}{273.2}\right)^{1.5}.$$

Thermal conductivity, W/(m·K):

$$\lambda_a=\lambda_{a0}\frac{273.2+C}{T+C}\left(\frac{T}{273.2}\right)^{1.5}.$$

C is the constant, which is almost independent of temperature and can be calculated using the formula $C=1.47T_{boil}$, where T_{boil} is the boiling temperature of the substance, K.

Multi-component mixture [19]: density:

$$\rho_{mix}=\rho_v\frac{P_v}{P}+\rho_a\frac{P-P_v}{P}.$$

Dynamic viscosity according to the formula, Pa·s:

$$\mu_{mix}=\frac{\mu_a}{1+\frac{x_v}{x_a}\Phi_{a,v}}+\frac{\mu_v}{1+\frac{x_a}{x_v}\Phi_{v,a}},$$

$$\Phi_{a,v}=\frac{\left[1+\left(\frac{\mu_a}{\mu_v}\right)^{0.5}\left(\frac{M_v}{M_a}\right)^{0.25}\right]^2}{2\sqrt{2}\left(1+\frac{M_a}{M_v}\right)^{0.5}},\quad \Phi_{v,a}=\frac{\left[1+\left(\frac{\mu_v}{\mu_a}\right)^{0.5}\left(\frac{M_a}{M_v}\right)^{0.25}\right]^2}{2\sqrt{2}\left(1+\frac{M_v}{M_a}\right)^{0.5}},$$

where $x_v=P_v/P$, $x_a=(P-P_v)/P$ – mole fraction of vapor and air.

Heat capacity:

$$c_{pmix}=c_{pv}\bar{C}_v+c_{pa}\left(1-\bar{C}_v\right),$$

where the dimensionless concentration of fuel vapor is:

$$\bar{C}_v = \frac{\rho_v \frac{P_v}{P}}{\rho_{mix}}.$$

Thermal conductivity according to the formula:

$$\lambda_{mix} = \frac{\lambda_a}{1+\frac{x_v}{x_a}A_{a,v}} + \frac{\lambda_v}{1+\frac{x_a}{x_v}A_{v,a}},$$

with the coefficients that were calculated by the formula:

$$A_{a,v} = \frac{1}{4}\left[1+\left[\frac{\mu_a}{\mu_v}\left(\frac{M_v}{M_a}\right)^{0.75}\cdot\frac{1+\frac{C_a}{T}}{1+\frac{C_v}{T}}\right]^{0.5}\right]^2\cdot\frac{1+\frac{C_{a,v}}{T}}{1+\frac{C_a}{T}},$$

$$A_{v,a} = \frac{1}{4}\left[1+\left[\frac{\mu_v}{\mu_a}\left(\frac{M_a}{M_v}\right)^{0.75}\cdot\frac{1+\frac{C_a}{T}}{1+\frac{C_v}{T}}\right]^{0.5}\right]^2\cdot\frac{1+\frac{C_{v,a}}{T}}{1+\frac{C_v}{T}},$$

where C_a, C_v are the constants, which can be calculated depending on the boiling temperatures of the components using the formula; $C_{a,v} = \sqrt{C_a C_v}$.

The thermodynamic parameters of the gas in the above-piston space depend on the degree of compression, which is determined by the volume of the charge:

$$V = \frac{\pi D_p^2}{4}\left(\frac{A}{2} - x\right) + V_{vch} - V_{sw},$$

where V is the volume of the charge in the space above the piston, m^3; D_p is the piston diameter, m; V_{vch}, V_{sw} are the volume of the vortex chamber and the swirl generator, m^3; A is the piston course, m; $x = (A/2)\sin\omega\tau$ is the distance from the cylinder head to the piston, m; $\omega = 2\pi n$ is the angular velocity of the shaft rotation, rad/s; τ is time, s; n is the number of shaft revolutions per unit of time, s^{-1}.

Then the compression ratio ε, pressure, and temperature are determined as:

$$\varepsilon = \frac{V^{l.d.p.}}{V}, P = P_0\varepsilon^{æ}, T = T_0\varepsilon^{æ-1},$$

where $V^{l.d.p.}$ is volume of the chamber, m^3; æ is adiabatic index.

The system of differential equations (14), (17), (18) was solved numerically using the fourth-order Runge-Kutta method.

3. Results and Discussion

Input data: motor fuel – diesel $d_4^{20} = 0.86$, $s_0 = 31\cdot10^{-3}$ N/m, $c_{f0} = 1.865$ kJ/(kg·K), fuel vapor – $D_{v0} = 7.3\cdot10^{-6}$ m^2/s, $c_{v0} = 1.6$ kJ/(kg·K), $P_{cr} = 1.35$ MPa; air – $M_a = 0.029$·kg/mole, $\mu_{a0} = 17.19\cdot10^{-6}$ Pa·s, $\lambda_{a0} = 2.44\cdot10^{-2}$ W/(m·K); normal conditions – $T_0 = 273.15$ K, $P_0 = 101325$ Pa.

The initial data for accounts: a diameter of the piston $D_n = 0.08$ m; course $A = 0.075$ m; $V^{l.d.p} = 391.5\cdot10^{-6}$ m^3; $V_{vch} = 20.4\cdot10^{-6}$ m^3; $V_{sw} = 5.87\cdot10^{-6}$ m^3; injection advance angle 26°; number of the crankshaft revolutions $n = 3000$ min^{-1}; æ = 1.4; degree of compression 19.3.

Chamber of combustion: volume of the chamber 20.6 sm^3, diameter 0.05 m, height $h = 7$ mm, $R_k = 22.5$ mm, $d = 20°$.

Initial conditions for the drops: $r_0/R_c = 0.2$, $z_0 = 0$, $V_0 = 0$, $W_0 = 11.6$ m/s, $U_0 = 4.7$ m/s, which are calculated according to [16].

The calculation of the motion and evaporation of droplets in the blind vortex chamber was used to determine the distribution of fuel vapor across the radius of the chamber. With the given dimensions of the vortex chamber, droplets with a diameter of up to 90.7 μm, inclusive, evaporate. This diameter is considered the maximum diameter of the monovariate distribution ($V = 0.95$; $\beta = 77.18$). The form of the integral function of the monovariate distribution V and the fuel volume v, which corresponds to the diameter intervals of droplets when dividing the spray spectrum 0–90.7 μm into $k = 20$ sections, is shown in Fig. 2.

When the spray cone angle exceeds 75°, the droplets do not reach the bottom of the vortex chamber. Due to evaporation from the droplets, their final temperature does not exceed 500–540 K, which is lower than the average boiling temperature of 556 K under normal conditions.

The distribution of the specific mass of fuel vapor across the radius of the chamber is shown in Fig. 4. The graphs indicate that, in the flat vortex chamber with the given dimensions, uniform distribution of fuel vapor in the air is not achieved.

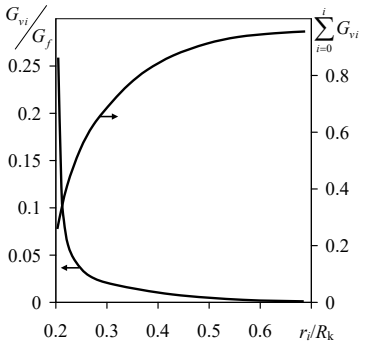

Fig. 4. The specific mass of fuel vapor across the radius of the chamber

The distribution of the specific air-fuel ratio across the radius of the combustion chamber is shown in Fig. 5.

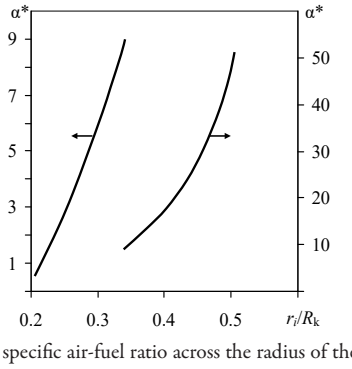

Fig. 5. The specific air-fuel ratio across the radius of the chamber

As expected, due to evaporation, the mass of the vapor rapidly increases, and at $r/R_c = 0.22$, the coefficient $\alpha^* = 1$, meaning that the air-fuel mass ratio is the same as that for the entire fuel in the chamber. Since the air temperature in the combustion chamber is determined by the degree of compression, and autoignition is influenced by the concentration of fuel vapor in the air, ignition is expected to occur at this radius. The evaporation of droplets, with the assumed atomization dispersion from the injector, finishes at a radius of $r/R_c \approx 0.8$. Thus, despite the significant non-uniformity of fuel vapor distribution across the radius, the combustion focus is formed in the majority of the combustion chamber, ensuring volumetric combustion of the fuel.

Practical significance. The created mathematical model can be used to calculate the geometric parameters of combustion chambers, select the dispersion, angle, initial velocity of nozzle droplets, and their operating mode to achieve volumetric mixing in internal combustion engines. The field of application is power engineering and thermal

ISSN-L 2664-9969; E-ISSN 2706-5448

power engineering, institutions engaged in the research, development, design and manufacture of combustion chambers.

Limitations of research. The above results assume that the spray is symmetrical around the Oz axis, a limitation that can be easily removed by adding another internal calculation loop to the program and setting the appropriate input data, but the result will be a significant increase in the overall calculation time.

Influence of martial law conditions. In the context of martial law and unstable power supply, this will require additional costs for calculations and equipment for uninterrupted power supply.

Prospects for further research. In the future, it is planned to create a universal software package taking into account various geometries for calculating the processes of hydro gas dynamics and thermochemical analysis in combustion chambers for a dispersed carbon-containing medium.

4. Conclusions

Based on the laws of motion and evaporation of droplet, a mathematical model has been developed, and calculations of the mixture formation process in a vortex combustion chamber located in the piston have been performed.

The distribution of the specific mass of fuel vapor and the specific air-fuel ratio along the radius of the combustion chamber has been determined. It has been shown that with the adopted droplet dispersion function of 0–90.7 μm, volumetric mixture formation is ensured, and the dimensionless air excess coefficient is achieved at $r/R_c = 0.22$. This is explained by the rapid evaporation of small droplets, the number of which, as a function of the diameter distribution, is the majority, and their high speeds of movement relative to air and, accordingly, high mass transfer coefficients in the initial spraying area.

The results can be used in the design of new diesel engines and to determine their operating modes.

Conflict of interest

The authors declare that they have no conflict of interest in relation to this research, including financial, personal, authorship or other, which could affect the research and its results presented in this article.

Financing

The research was conducted without financial support.

Data availability

The manuscript has no associated data.

Use of artificial intelligence

The authors confirm that they did not use artificial intelligence technologies when creating the presented work.

References

1. Changxiong, L., Hu, Y., Yang, Z., Guo, H. (2023). Experimental Study of Fuel Combustion and Emission Characteristics of Marine Diesel Engines Using Advanced Fuels. *Polish Maritime Research, 30 (3),* 48–58. https://doi.org/10.2478/pomr-2023-0038
2. Elkelawy, M., Alm ElDin Mohamad, H., Abd Elhamid, E., El-Gamal, M. (2022). A critical review of the performance, combustion, and emissions characteristics of PCCI engine controlled by injection strategy and fuel properties. *Journal of Engineering Research, 6 (5).* https://doi.org/10.21608/erjeng.2022.168050.1108
3. Smyth, T., Jaspers, I. (2024). Diesel exhaust particles induce polarization state-dependent functional and transcriptional changes in human monocyte-derived macrophages. *American Journal of Physiology-Lung Cellular and Molecular Physiology, 326 (1),* L83–L97. https://doi.org/10.1152/ajplung.00085.2023
4. Long, E., Carlsten, C. (2022). Controlled human exposure to diesel exhaust: results illuminate health effects of traffic-related air pollution and inform future directions. *Particle and Fibre Toxicology, 19 (1).* https://doi.org/10.1186/s12989-022-00450-5
5. Richard, P. (2024). *Feynman Center for Innovation. KIVA*. Available at: https://www.lanl.gov/engage/collaboration/feynman-center
6. AVL FIRE™ M. *Simulations That Challenge Reality.* Available at: https://www.avl.com/en/simulation-solutions/software-offering/simulation-tools-a-z/avl-fire-m
7. *VECTIS.* Realis Simulation. Available at: https://www.realis-simulation.com/insights/brochures/vectis/
8. *ANSYS.* Available at: https://www.ansys.com
9. Millo, F., Piano, A., Roggio, S., Pastor, J. V., Micó, C., Lewiski, F. et al. (2022). Mixture formation and combustion process analysis of an innovative diesel piston bowl design through the synergetic application of numerical and optical techniques. *Fuel, 309,* 122144. https://doi.org/10.1016/j.fuel.2021.122144
10. Yazar, O., Demir, B. (2022). Development of the Software Program That Can Account the Combustion, Emission and Engine Performance Values of Internal Combustion Engines. *European Journal of Technic, 12 (2),* 129–136. https://doi.org/10.36222/ejt.1147020
11. Wang, D., Shi, Z., Yang, Z., Chen, H., Li, Y. (2022). Numerical study on the wall-impinging diesel spray mixture formation, ignition, and combustion characteristics in the cylinder under cold-start conditions of a diesel engine. *Fuel, 317,* 123518. https://doi.org/10.1016/j.fuel.2022.123518
12. Strauß, L., Rieß, S., Wensing, M. (2023). Mixture formation of OME3-5 and 1-Octanol in comparison with diesel-like Dodecane under ECN Spray A conditions. *Frontiers in Mechanical Engineering, 9.* https://doi.org/10.3389/fmech.2023.1083658
13. Xiang, L. W., Sapit, A., Azizul, M. A., Darlis, N., Abidin, S. F. Z., Ismail, M. M., Andsaler, A. (2023) Effect of High Ambient Temperature and Pressure on Spray Penetration Length Using Computational Fluid Dynamics. *Fuel, Mixture Formation and Combustion Process, 5 (1).*
14. Nur Syuhada, M. Y., Norrizam, J., Shaiful Fadzil, Z., Imadduddin, R., Muhammad Nazif, M., Norrizal, M. et al. (2023). Combustion Strategies in Controlling the Combustion Process and Emission for Internal Combustion Engines: A Review. *Fuel, Mixture Formation and Combustion Process, 5 (2).*
15. Koval, V. P., Al Rusan, A. A. (2003). Pat. 56266 UA. *Kamera zghoriannia dyzelnoho dvyhuna.* MPK: F02B 23/04. published: 15.05.2003, Bul. No. 5.
16. Al Rusan, A. A. D. (2003). *Obiemne sumishoutvorennia u vykhrovii kameri, yaka zapovniuietsia.* [Dysertatsiia na zdobuttia stupenia kandydata nauk; Natsionalna metalurhiina akademiia Ukrainy].
17. Raushenbakh, B. V., Belyy, S. A., Bespalov, I. V., Borodachev, V. Ya., Volynskiy, M. S., Prudnikov, A. G. (1967). *Physical principles of the working process in combustion chambers of jet engines.* Wright-Patterson Air Force Base, FTD-MT-65–78.
18. Koval, V. P., Al Rusan, A. A. (2002). Dvizhenie ispariaiushchikhsia kapel v glukhoi vikhrevoi kamere sgoraniia porshnia dizelnogo DVS. *Integrirovannye tekhnologii i energosberezhenie, 4,* 59–66.
19. Bretsznajder, St. (1962). *Własności gazów i cieczy*. Warszawa: Wydawnictwa Naukowo-Techniczne.

Oleksandr Zhevzhyk, *PhD, Associate Professor, Department of Intelligent Power Supply Systems, Ukrainian State University of Science and Technologies, Dnipro, Ukraine, ORCID: https://orcid.org/0000-0002-8938-9301*

✉***Iryna Potapchuk,*** *PhD, Associate Professor, Department of Intelligent Power Supply Systems, Ukrainian State University of Science and Technologies, Dnipro, Ukraine, e-mail: i.y.potapchuk@ust.edu.ua, ORCID: https://orcid.org/0000-0002-5985-1040*

Vadym Horiachkin, *PhD, Associate Professor, Head of Department of Computer and Information Technology, Ukrainian State University of Science and Technologies, Dnipro, Ukraine, ORCID: https://orcid.org/0000-0002-8952-952X*

Serhii Raksha, *Doctor of Technical Sciences, Professor, Head of Department of Applied Mechanics and Materials Science, Ukrainian State University of Science and Technologies, Dnipro, Ukraine, ORCID: https://orcid.org/0000-0002-4118-1341*

Dmytro Bosyi, *Doctor of Technical Sciences, Professor, Head of Department of Intelligent Power Supply Systems, Ukrainian State University of Science and Technologies, Dnipro, Ukraine, ORCID: https://orcid.org/0000-0003-1818-2490*

Andrii Reznyk, *Director, Limited Liability Company "PromSpecEngineering", Dnipro, Ukraine, ORCID: https://orcid.org/0009-0001-8825-2186*

✉*Corresponding author*